es101771g

DATASET · MAY 2014

2 AUTHORS:

Zuohao Cao
Environment Canada, Toronto, Ontario
41 PUBLICATIONS **332** CITATIONS

SEE PROFILE

Jianmin Ma
Lanzhou University
79 PUBLICATIONS **1,384** CITATIONS

SEE PROFILE

Quantifying the Perturbations of Persistent Organic Pollutants Induced by Climate Change

JIANMIN MA*,† AND ZUOHAO CAO‡

Air Quality Research Division, Environment Canada, 4905 Dufferin Street, Toronto, Ontario M3H 5T4, Canada, and Meteorological Service of Canada, 4905 Dufferin Street, Toronto, Ontario M3H 5T4, Canada

A perturbed air–surface coupled model has been developed to simulate and predict perturbations of POPs concentrations in various environmental media under given climate change scenarios. By introducing the perturbations in air temperature and precipitation induced by climate change in the model, we have examined the corresponding perturbations in the concentration of POPs in the closed air–soil and air–water systems. Numerical experiments for several POPs have been conducted based on the possible future climate change scenarios. It was found that hexachlorobenzene (HCB), hexachlorocyclohexanes (HCHs), and a polychlorinated biphenyl (PCBs) congener, PCB-153, exhibit strong response to specified climate change scenarios as shown by their high concentrations perturbations in air. In the air–soil system the coupled model predicts 4–50% increases in the air concentrations of these chemicals corresponding to an increase of 0.05–0.1 K yr^{-1} in the air temperature. Based on our simulations, a 20% increase/decrease in precipitation can result in a 53% and 4% decrease/increase in perturbed air concentration of γ-HCH and α-HCH, respectively. Also, the model can be used to determine the direction of air–surface exchange of POP perturbations induced by climate change.

Introduction

Persistent organic pollutants (POPs) in air, water, soil, vegetation, snow, and ice are connected by a set of exchange and transport pathways among these reservoirs. Under the direct influence of climate change (change in temperature and precipitation), these reservoirs have been undergoing significant changes (*1*). Concerns have been raised in the last several years that climate warming would very likely increase exposure of the environment and ecosystem to POPs (*2–5*). Observational and modeling evidence also revealed connections between climate change/variability and POPs in the environment (*6–13*). In the case of the major legacy POPs, large quantities (in the order of kilo- to megatons) have been released into the environment in the last half century (*14*), much of which now resides in the soil, water, vegetation, and snow/ice reservoirs. These reservoirs, as secondary emission sources, have become dominant sources for some of the banned POPs, e.g., HCHs, and are easily

affected by changes in environmental parameters like temperature, precipitation, and winds (*4*).

Although efforts have been made in the past decade to assess and evaluate the impact of climate change and variation on the environmental exposure to POPs, there is a growing need to quantify the change in the magnitude and direction of POPs exchange between different reservoirs induced by climate change. Sophisticated general circulation models (GCM) have been extensively used to project the impact of regional and global climate change on environmental systems (*1*). Only a few studies have used a modeling approach to predict the environmental fate of POPs subject to climate change scenarios (*9, 12, 13*). By projecting the change in atmospheric conditions (e.g., air temperature, precipitation, winds) under climate change scenarios, these studies examined changes in atmospheric concentration levels of POPs. However, uncertainties still remain in understanding the interactions between climate change and environmental fate of POPs. Although the response of POPs to projected climate change scenarios was inferred through the response of chemical/physical properties of POPs to changes in temperature and precipitation in these modeling investigations, such response was not quantified. It is also interesting to extract and quantify climate signals in POPs concentrations in multicompartment environments, for instance, climate driven residence time, long-range transport potential, and temporal trend.

This study develops a perturbation model for POPs concentrations in multi environmental compartments to quantify changes in concentration of POPs in these compartments subject to fluctuating air temperature and precipitation induced by climate change. Perturbation analysis is useful for understanding the important processes affecting pollutant concentrations (*15*). The perturbation approach has been used in chemical transport models (CTM) to investigate the impact of climate change on air quality through perturbing individual meteorological variables in a CTM. The present study introduces a new perturbation approach to a two-box model for POPs. The aim of the study is to provide a simple model to evaluate and screen the influence of future climate change on POPs dynamics and environmental fate. The effect of the change in winds on POPs environmental fate is not taken into account in the present study because the perturbation model focuses only on a closed two-compartment system in which atmospheric transport is not taken into account.

Methodology

In this section we shall present the derivation of the perturbation model in air–soil and air–water systems and also model solutions with certain initial conditions. We start from a closed two-compartment system that has been used to compute exchange and transport of POPs between and within the system (*16, 17*)

$$\frac{dc_a}{dt} = -a_1 c_a + b_1 c_s \qquad (1)$$

$$\frac{dc_s}{dt} = a_2 c_a - b_2 c_s \qquad (2)$$

where c_a and c_s are concentration of a persistent chemical in air and a surface compartment, respectively. For the air–soil system, the coefficients in eqs 1 and 2 are defined as

---

* Corresponding author e-mail: jianmin.ma@ec.gc.ca.
† Environment Canada.
‡ Meteorological Service of Canada.

$$a_1 = \left(\frac{(1 - \phi_{air})(v_a + v_d)}{z_a} + \lambda_a + k_a \right) \tag{3a}$$

$$a_2 = \frac{(1 - \phi_{air})(v_a + v_d)}{z_s} + \lambda_s \tag{3b}$$

$$b_1 = \frac{v_s}{z_a K_{sa}} \tag{3c}$$

$$b_2 = \left(\frac{v_s}{z_s K_{sa}} + k_s \right) \tag{3d}$$

For the air–water system, these coefficients are defined by (17, 18)

$$a_1 = \left(\frac{(1 - \phi_{air})(v_a + v_d)}{z_a k_{aw}} + \lambda_a + k_a \right) \tag{3e}$$

$$a_2 = \frac{(1 - \phi_{air})(v_a + v_d)}{z_s k_{aw}} + \lambda_s \tag{3f}$$

$$b_1 = \frac{v_s}{z_a} \tag{3g}$$

$$b_2 = \left(\frac{v_s}{z_s} + k_o \right) \tag{3h}$$

In eqs 3a–h, K_{sa} is air–soil partition coefficient and K_{aw} is air–water partition coefficient, v_a is the mass transfer coefficient from air to surface (or gas phase diffusive exchange velocity, m s^{-1}), and v_s is the mass transfer coefficient from surface to air (m s^{-1}). In this study we have assumed $v_s = v_a$ in both air–soil and air–water systems. v_d is the dry particle deposition velocity (m s^{-1}) and ϕ_{air} is the particle-bound fraction in air, defined in Supporting Information (SI). In eq 3a z_a and z_s (m) are the atmospheric height and the depth of a surface compartment between which the exchange and transfer of the chemical take place. k_a and k_s (k_o) are degradation rate constants (s^{-1}) in air and surface (soil and water) compartment, $\lambda_a = W P_I / z_a$ (s^{-1}) in eqs 3a and 3e, and $\lambda_s = W P_I / z_s$ (s^{-1}) in eqs 3b and 3f are the scavenging coefficients where W is the washout ratio and P_I is the precipitation (mm yr^{-1}). The mean and perturbation of these parameters are presented in SI as well. The total degree of scavenging of a given compound can be expressed by $W = W_g(1 - \phi_{air}) + W_p \phi_{air}$ (17), where W_g is the washout ratio for the gaseous fraction of the compound and W_p is the particle washout ratio, respectively. The process of wet particle deposition is considered more important than dry deposition (19). Because W_p is often taken as a constant from experiments or measurements but seems not to depend explicitly on a meteorological variable (20), it is assumed to not vary with climate change scenarios and hence is not considered further in this study.

As shown in eqs 1 and 2, the model consists of two compartmental boxes, one in the air at concentration c_a, the other immediately below it in the underlying surface compartment at concentration c_s. The response of persistent chemicals to climate change involves the response of chemical/physical processes described above to the changes in air temperature and precipitation. In atmospheric science and climate research a climate perturbation can be denoted as a departure of air temperature from its mean (e.g., 21, 22), $T = \bar{T} + T'$, where T is air temperature (K), $\bar{T}$ is the time-invariant (decadal or longer) mean air temperature, and T' is the departure from the mean or air temperature (climate) perturbation. Using this approach with a prime denoting perturbation we can also define

$$c_a = \bar{c}_a + c'_a \tag{4a}$$

$$c_s = \bar{c}_s + c'_s \tag{4b}$$

in which the concentration of chemicals in air and surface compartments is equal to the sum of mean concentration and perturbed concentrations by climate change. To find these perturbed concentrations induced by climate change, we employed a perturbation method (23). The perturbation theory requires that a mean concentration must satisfy the mean concentration equations, and that the perturbation must be small enough, so that all terms in the governing equations that involve products of the perturbations can be neglected. In the case of POPs concentrations in the air and surface medium, this suggests that $\bar{a} c' \gg a' c'$, where a is a model coefficient. Because the perturbation of a quantity is at least 1 order of magnitude smaller than its mean, the product of two perturbed quantities becomes a high order perturbation, and hence can be neglected. Following these rules and substituting eqs 4a and 4b into eqs 1 and 2 we arrive at two equations for concentration perturbations in the air and surface compartments, respectively

$$\frac{dc'_a}{dt} = -\bar{a}_1 c'_a + \bar{b}_1 c'_s + d_1 \tag{5}$$

$$\frac{dc'_s}{dt} = \bar{a}_2 c'_a - \bar{b}_2 c'_s + d_2 \tag{6}$$

where

$$d_1 = -a'_1 \bar{c}_a + b'_1 \bar{c}_s \tag{7a}$$

$$d_2 = a'_2 \bar{c}_a - b'_2 \bar{c}_s \tag{7b}$$

In eqs 5–7, $\bar{a}_1$, $\bar{a}_2$, $\bar{b}_1$, $\bar{b}_2$, a'_1, a'_2, b'_1, and b'_2 are the mean and perturbed coefficients a_1 and a_2 defined in eqs 3a and b, and b_1 and b_2. The means and perturbations of these coefficients and their expressions are presented in SI. In deriving eqs 5 and 6, we have eliminated high order perturbations $a'_1 c'_a$, $b'_1 c'_s$, $a'_2 c'_a$, and $b'_2 c'_s$ following the rules in the perturbation analysis. In principle, a mean variable is a time-invariant quantity, so that $d\bar{c}/dt = 0$ and $\bar{c} = $ const. In the first instance, we shall assume constant concentrations in air and surface compartments. However, considering the evidence of declining trend of POPs after their phase out (10, 11), we shall subsequently relax this assumption by introducing a slowly varying mean concentration in air and surface media into the perturbation model.

To pursue a mathematical solution for concentration perturbation in air only, taking derivative of eq 5 with respect to time t and eliminating dc_s'/dt by combining the resulted equation with eq 6, we obtain a perturbation equation for air concentration as

$$\frac{d^2 c'_a}{dt^2} + \alpha \frac{dc'_a}{dt} + \beta c'_a = \Gamma \tag{8}$$

where

$$\alpha = \bar{a}_1 + \bar{b}_2, \beta = \bar{a}_1 \bar{b}_2 - \bar{a}_2 \bar{b}_1, \text{ and } \Gamma = \bar{b}_1 d_2 + \bar{b}_2 d_1 \tag{9}$$

Equation 8 is a second order nonhomogeneous equation with constant coefficients for the concentration perturbation. The nonhomogeneous term Γ on the right-hand side of eq 8 is a *forcing* term relating to mean concentrations in air and surface compartments (eqs 7a and b) and exchange processes between the two boxes (eq 3). Because α and β are not functions of time but depend only on mean air temperature

and precipitation, an exact solution to eq 8 is straightforward under the initial conditions $c'_a(t = 0) = 0$ and $dc'_a/dt\ (t = 0) = 0$, expressed as (see SI for details)

$$c'_a(t) = \frac{\Gamma}{\beta(r_1 - r_2)}[(r_1 - r_2) + r_2 e^{r_1 t} - r_1 e^{r_2 t}] \qquad (10)$$

where

$$r_1 = \frac{-\alpha + \sqrt{\alpha^2 - 4\beta}}{2} \qquad (11a)$$

$$r_2 = \frac{-\alpha - \sqrt{\alpha^2 - 4\beta}}{2} \qquad (11b)$$

Substituting eq 10 into eq 6 and integrating the resulting equation with respect to time t we can derive the concentration perturbation in the surface compartment (details are given in SI)

$$c'_s(t) = \frac{1}{\bar{b}_2}\left(d_2 + \frac{\bar{a}_2 \Gamma}{\beta}\right) + \frac{\bar{a}_2 \Gamma}{\beta(r_1 - r_2)}\left(\frac{r_2}{r_1 + \bar{b}_2}(e^{r_1 t} - e^{-\bar{b}_2 t}) - \frac{r_1}{r_2 + \bar{b}_2}(e^{r_2 t} - e^{-\bar{b}_2 t})\right) \qquad (12)$$

To relax constant mean concentration hypothesis, we now assume that the mean concentrations vary exponentially with the mean degradation rate constants in the air and surface compartments, namely,

$$\bar{c}_a = \bar{c}_{a0}\exp(-\bar{k}_a t) \qquad (13a)$$

and

$$\bar{c}_s = \bar{c}_{s0}\exp(-\bar{k}_s t) \qquad (13b)$$

This assumption applies in a closed environment without physical removal, i.e., nonreactive losses (24). This implies that the air concentration is also subject to change without degradation if the system is far from equilibrium (or from steady-state). In this case, one may use the removal rate (residence time) derived from the "temporal remote state" or overall persistence in terms of degradations in multicompartments and phase partitioning, so that $k_a = k_s = k_{ov} = 1/\tau^{rs}$, where τ^{rs} is overall persistence (24−26) and k_{ov} is the removal rate due to overall persistence. Calculations demonstrate that the adoption of k_{ov} results in faster decline, or less slowly varying, of the mean air concentrations of POPs compared with that derived from eq 13a. As a result, the faster decline (variation) in the mean concentrations may overwhelm perturbed concentrations, so that climate change signals in the perturbed concentrations become less clear. This suggests that the mean concentrations should be taken, whenever possible, as a time-invariant quantity or a slowly varying variable following the rules in the perturbation analysis, enabling perturbed concentrations induced by climate scenarios to be more clearly illustrated.

Putting eq 13a into eq 7a and Γ the solution 10 of eq 8 under the same initial conditions can be extended as

$$c'_a(t) = \frac{1}{r_1 - r_2}[(F_1 r_2 + F_2)e^{r_1 t} - (F_1 r_1 + F_2)e^{r_2 t}] + B_1 e^{-\bar{k}_a t} + B_2 e^{-\bar{k}_s t} \qquad (14)$$

where

$$A_1 = \bar{c}_{a0}(\bar{b}_1 a'_2 - \bar{b}_2 a'_1) \qquad (15a)$$

$$A_2 = \bar{c}_{so}(\bar{b}_2 b'_1 - \bar{b}_1 b'_2) \qquad (15b)$$

$$F_1 = B_1 + B_2 \qquad (16a)$$

$$F_2 = k_a B_1 + k_s B_2 \qquad (16b)$$

and

$$B_1 = \frac{A_1}{r_1 - r_2}\left(\frac{1}{k_a + r_2} - \frac{1}{k_a + r_1}\right) \qquad (17a)$$

$$B_2 = \frac{A_2}{r_1 - r_2}\left(\frac{1}{k_s + r_2} - \frac{1}{k_s + r_1}\right) \qquad (17b)$$

Accordingly, the concentration perturbation in the surface compartment is given by

$$c'_s(t) = \frac{d_2}{\bar{b}_2} + \frac{\bar{a}_2}{r_1 - r_2}\left[\frac{F_1 r_2 + F_2}{r_1 + \bar{b}_2}(e^{r_1 t} - e^{-\bar{b}_2 t}) - \frac{F_1 r_1 + F_2}{r_2 + \bar{b}_2}(e^{r_2 t} - e^{-\bar{b}_2 t})\right] + \frac{B_1}{\bar{b}_2 - k_a}(e^{-\bar{k}_a t} - e^{-b_2 t}) + \frac{B_2}{\bar{b}_2 - k_s}(e^{-\bar{k}_s t} - e^{-\bar{b}_2 t}) \qquad (18)$$

It should be noted that, differing from those positively defined mean variables and parameters (e.g., concentrations), their perturbations can be either positive or negative in the perturbation analysis. Equations 10, 12, 14, and 18 indicate that the concentration perturbations in both compartments are expressed by simple elementary functions, so that their computations are easily carried out. Once the mean concentrations, mean air temperature, mean precipitation, and perturbed air temperature and precipitation due to climate change are given, the perturbations of POPs in air and surface compartments can be derived from eqs 10, 12, 14, and 18.

Results and Discussion

Numerical experiments have been carried out for five chemicals to demonstrate the change in concentrations of these chemicals in air and surface compartments induced by climate change. These chemicals are α- and γ-HCHs, HCB, and PCB-28 and -153. Their chemical/physical properties and environmental parameters are listed in Tables S1−S3 of SI. Because long-term time series of measured POPs air concentration are rare, data on the five selected chemicals in air, water, and soil were collected from literature and field measurements and are listed in Table S4 of SI. Note that these data are not long-term mean concentrations. Therefore, the following results present to some extent a conceptual demonstration of the model's capability in predicting the influence of climate change on POPs levels in the environment. The mean air temperature T and mean annual precipitation are taken as 283 K and 800 mm yr^{-1} respectively. These values have been observed often in midlatitudes in the Northern Hemisphere (27). We first take a perturbation of precipitation as 80 mm yr^{-1}, or 10% of the mean. We then implement a perturbed precipitation of 160 mm yr^{-1} as the climate change induced precipitation anomaly (1) in the model in the air−soil system, to demonstrate the model capability in quantifying the response of POPs to climate induced precipitation anomalies. Results are presented in Section 5 and Figure S1 of SI. The perturbations of chemical/physical properties (Henry's law constant, log K_{OA}, degradation rate constants, etc.) and model coefficients (a'_1, a'_2, b'_1, and b'_2) of the selected chemicals subject to temperature perturbations are illustrated in Figures S2 and S3 and discussed in SI. Several case studies have been carried out
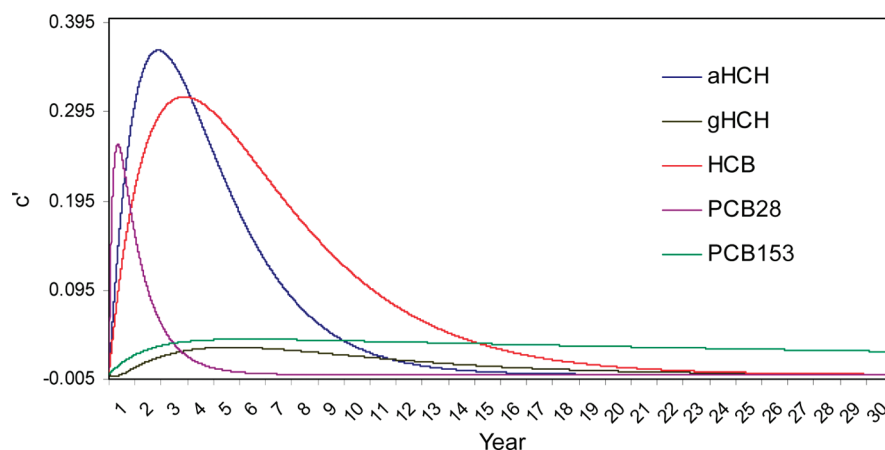
FIGURE 1. Simulated concentration perturbations (pg m^{-3}) of selected chemicals in air for a 30-year period. Mean air and water concentrations are listed in Table S4 of SI. Mean and perturbed air temperature are taken as 283 K and 0.1 K yr^{-1}, respectively.
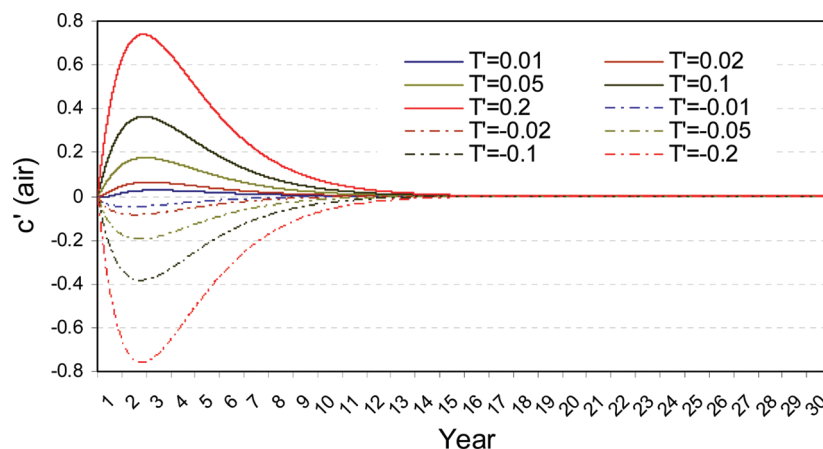

FIGURE 2. Simulated perturbed air concentration (pg m^{-3}) of α-HCH under different cooling and warming conditions.

to evaluate the change in concentrations of the selected chemicals in air and surface compartments.

Air–Water. The mean concentration values of the selected chemicals in air (pg m^{-3}) and water (ng L^{-1}) (Table S4 of SI) show revolatilization from water to air, calculated from water–air exchange flux (*18*), except for γ-HCH which shows deposition. In the first experiment, the temperature perturbation of 0.1 K yr^{-1} is employed in the model for all chemicals. Simulated concentration perturbations in air are displayed in Figure 1 and concentration perturbations in water are plotted in Figure S4 of SI. As shown in Figure 1, α-HCH, HCB, and two PCBs exhibit positive perturbation (pg m^{-3}) in the atmosphere throughout the 30-year period, reaching the maximum at about 2 years and subsequently a steady-state after 15 years model integration. γ-HCH shows negative concentration perturbations for the first year, forced by deposition of the mean concentration from air to water, and a negative to positive perturbation reversal thereafter. Though the perturbations in water are less compared to those in air, especially for PCBs, the perturbations in water show a trend opposite that in air (Figure S4), suggesting a loss of the chemicals in water compared to the gain in the air due to volatilization under the warming condition.

Figure 2 illustrates the change in the concentration perturbation of α-HCH in air subject to different temperature perturbations from −0.2 to 0.2 K yr^{-1}, representing cooling and warming climate scenarios. For instance, the selected warming conditions of 0.02 and 0.05 K yr^{-1} are within the range of the IPCC global warming scenarios (*1*). As expected, concentration perturbations increase/decrease with increasing/decreasing air temperature perturbations, and positive

and negative temperature perturbations lead to a symmetric pattern of positive and negative concentration perturbations.

Air–Soil. Three case studies are presented in this section. First, we examine perturbed concentration of the selected chemicals in the closed air–soil system under a temperature perturbation $T' = 0.05$ K yr^{-1} and a precipitation perturbation at 80 mm yr^{-1}. Mean air and soil concentrations of the selected chemicals are listed in Table S4 of SI. These mean concentration values yield revolatilization from soil to air for the all chemicals as characterized by a soil/air fugacity ratio $f_S/f_A > 1$. Simulated concentration perturbations according to eq 10 over the 30-year period under these conditions and constant mean air and soil concentrations (without degradation) are illustrated in Figure S5 of SI. Strong perturbation induced by $T' = 0.05$ K yr^{-1} occurs for HCB, primarily due to its stronger volatilization from soil to air. The perturbation reaches a steady state after 15 years integration at about $c' = 19$ pg m^{-3}, or a 32% increase to the mean air concentration of 60 pg m^{-3} under the warming condition. Strong link between HCB and interannual climate variability (air temperature) has been revealed previously (*7, 11*). Measured HCB annual averaged air concentrations in the vicinity of the Great Lakes were found to increase dramatically in 1997 and 1998 when a strong El Nino event occurred. Compared to the annual concentration values measured in the mid-1990s, the increase in the mean annual air concentration in 1998 was as high as 73%! Such a dramatic increase of HCB atmospheric level over the Great Lakes has been attributed to anomalous increase in the mean air temperature over Canadian Prairies and the west Great Lakes region from autumn 1997 through spring 1998 associated with this El Nino event, which led to strong volatilization of HCB from previously contaminated
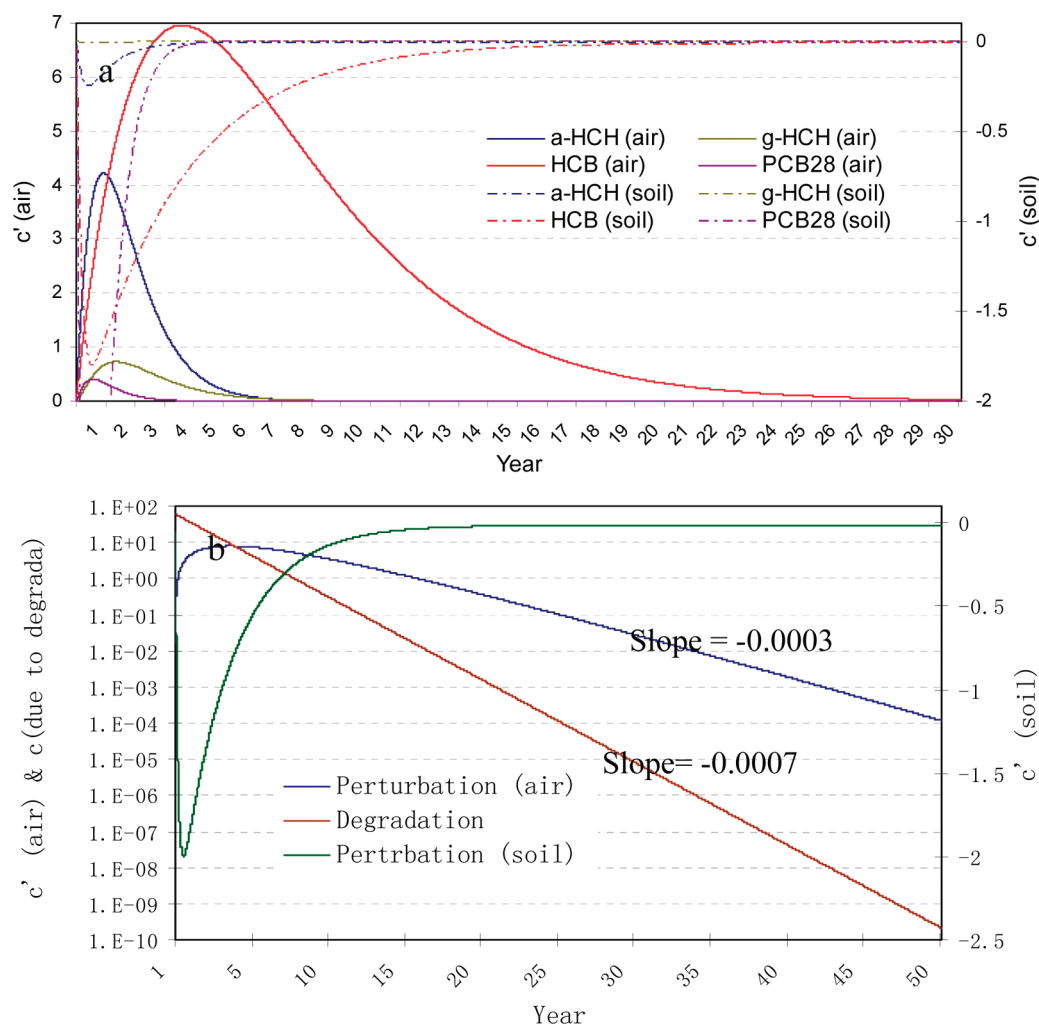
FIGURE 3. (a) Simulated concentration perturbations of HCHs, HCB, and PCB-28 in air (pg m^{-3}) and soil (μg kg^{-1}) according to eq 14 for a 30-year period. Mean air and soil concentrations in computations are listed in Table S4 of SI. Other conditions are the same as those used in Figure 1. Solid lines are for air concentration perturbation and dashed line is for soil concentration perturbation. **(b)** Simulated mean air concentration of HCB for a 50-year period due to degradation under $T = 283$ K. Other conditions are the same as those used in Figure 1a. Mean air concentrations subject to degradation and concentration perturbations (pg m^{-3}) are scaled logarithmically on the left axis and concentration perturbation in soil (ng kg^{-1}) is scaled on the right Y-axis.

soils over these regions (7). Annual perturbation of α-HCH in the air under the same warming condition (0.05 K yr^{-1}) is about 9.6 pg m^{-3} after it reaches a steady state, or a 23% increase compared to the mean air concentration of 40 pg m^{-3}. Compared with HCB, it takes less than 3 years for the perturbed α-HCH to increase from their initial value of zero to their quasi-steady state level. γ-HCH and PCB-28 exhibit a trend similar to that of α-HCH, showing an increase of 4% and 2% from their means (Table S4 of SI), respectively. Perturbed air concentration of PCB-153 shows a monotonically increasing trend and reaches 0.58 pg m^{-3} after 30 years integration, indicating an increase of 58% to its mean concentration (1 pg m^{-3}). This increasing trend can also be observed in Figure S6a of SI which illustrates simulated perturbations of PCB-153 in air and soil according to eqs 13a$-$18. If we extend model integration to 100 years, the perturbed air concentration exceeds its mean value of 1 pg m^{-3} (Figure S6b). However, forced by the degraded mean concentration in air and soil (eq 13a and b), the modeled perturbation starts to decline after 53-year integration (Figure S6b).

Figure 3a presents simulated perturbations of HCHs, HCB, and PCB-28 in air (pg m^{-3}) and soil (μg kg^{-1}) according to eq 14 under the warming condition of 0.1 K yr^{-1} and perturbed precipitation at 80 mm yr^{-1}, taking into account the mean degradation rate in air and soil given by eq 13a and b under the mean air temperature of 283 K and mean precipitation

800 mm yr^{-1}. Compared with Figure S5 derived from eq 10, there exists no steady state in the perturbed air concentrations of the chemicals. Except for PCB-153 as discussed above, perturbed HCB reaches the maximum after 5 years integration at about $c_a' \approx 7$ pg m^{-3}, followed by α-HCH ($c_a' \approx 4$ pg m^{-3}), γ-HCH ($c_a' = 0.7$ pg m^{-3}), and PCB-28 ($c_a' = 0.4$ pg m^{-3}) after 2 years integration. These results suggest that the warming condition at $T' = 0.1$ K yr^{-1} and the perturbed precipitation at 80 mm yr^{-1} results in maximum 12% increase of HCB and 10% increase of α-HCH in a single year. Following the increases during the first several years, the perturbed atmospheric concentrations tend to decrease due to degradation thereafter. Analogous to the results in air$-$water system shown in Figure 1, the simulated concentration perturbations in soil (μg kg^{-1}) exhibit opposite trend during the first several years, indicating revolatilization, and tend to diminish thereafter due to their degradation in soil. The perturbation of the selected chemicals (except for γ-HCH) in soil appears very strong due to model spin-up in the early stage of integration with absolute values of the perturbation even greater than its mean soil concentration, but tends to a steady-state thereafter. A similar trend is observed for perturbed concentrations of PCB-153 in air and soil (Figure S6a). Figure 3b further shows the comparison between concentration perturbations of HCB in air and soil and the

temporal trend of the mean air concentration due to degradation for a 50-year period. While the highest concentration perturbation is about 12% of the mean air concentration (60 pg m^{-3}), the mean air concentration is reduced so quickly by degradation that, after 6 years integration, it becomes lower than perturbed concentration induced by the temperature perturbation of 0.1 K yr^{-1}. This is also demonstrated by the steeper slope of the mean air concentration compared to the perturbed concentration, indicating that climate warming exerts a strong influence on the environmental fate of POPs.

Discussion. Strong responses of the selected chemicals to projected climate change scenarios are found for HCHs, HCB, and PCB-153. Change in the perturbed air concentrations of these chemicals in the air–soil system is 1 order of magnitude greater than that in the air–water system under the same warming condition. HCB exhibits largest perturbation in the air–soil system whereas α-HCH demonstrates the largest perturbation in the air–water system. While smaller octanol–air partition coefficient leads to stronger revolatilization of HCB from soil to air, the smaller Henry's law constant of α-HCH favors its revolatilization from water to air. Because of temperature dependence of the Henry's law constant (eqs S-11 and S-12 of SI), perturbed air concentration of α-HCH can increase or decrease 1 order of magnitude when subject to changes in the perturbed air temperature, as shown in Figure 2. Temperature cycles alter the partitioning (and vapor pressure) and chemicals will be more or less prone to revolatilization depending on how their intermedia distributions and equilibrium status are affected by the temperature cycles. Warming generally favors the vapor phase of POPs. Under warming conditions, POPs will be more prone to move again after deposition, to associate less with particles. Likewise, partitioning from air into water is also a function of temperature. Chemicals like HCHs, which partition strongly into water and whose partitioning is a strong function of temperature, will attempt to readjust their partitioning if the warming condition occurs, generally with the chemical being forced back into the atmosphere. Furthermore, the magnitude of a chemical's mean concentration in air and surface media determines initially the mean equilibrium status between the air and surface compartment which exerts a strong influence on its perturbation. For instance, the selected mean air and water concentration of γ-HCH (Table S4 of SI) leads to deposition from air to water which forces a negative perturbation of the chemical in the air for the first half year of integration. A negative to positive reversal of the exchange takes place after 10 years integration due to faster degradation process of γ-HCH in the air but the negative to positive reversal of perturbed air concentration occurs after merely a half year integration. This suggests high sensitivity and quick response of POPs to climate change. Slow decline of perturbed HCB in air (Figure 3b) as compared to the decrease of the mean air concentration induced by degradation suggests that the expected decline in the ambient atmospheric level of POPs is likely to slow down due to re-emission from other reservoirs accumulated during past use under warming climate.

Compared to PCB-28 the more pronounced response of PCB-153, particularly in the air–soil system, to the projected temperature perturbations is observed. In their modeling investigation, Lamon et al. (*12*) found a stronger response of PCB-153 to temperature changes than that of PCB-28 to temperature changes. Lamon et al. have validated their results against observations and attributed this result to the stronger primary emission of PCB-153 associated with larger absolute value of the internal energy of vaporization of this PCB congener. Primary emissions have not been taken into account in the present study. The monotonic increasing trend of PCB-153 derived from this study (Figure S6 of SI) is the result of evaporation from its abundance in the soil (2 μg kg^{-1}, Table S4 of SI). Because as a heavier PCB congener PCB-153 tends to deposit more quickly into soils, the greater abundance of PCB-153 in the soil may likely be associated with its primary emission rate. In SI (section 3.2) we have discussed a method to implement a primary emission into the perturbation model. Results indicate that perturbed air concentration of PCB-28 increases considerably when its primary emission is taken into account. Nevertheless, the simulated PCB-28 with the primary emission exhibits similar temporal pattern as shown in Figure 3a (see SI for details).

Uncertainties and Application. Since the model is derived from the exact solution of the air–surface systems, uncertainties in simulated concentration perturbations lie largely in estimating mass transfer coefficients, partitioning coefficients, and removal rate, as well as their perturbations. For example, the mean and perturbed mass transfer coefficient defined by eq S-10 of SI differ only by the mean and perturbed dimensionless Henry's law constant. However, because the air diffusion coefficient is 4 orders of magnitude greater than the liquid diffusion coefficient (Table S1), the air diffusion coefficient dominates the mass transfer coefficient while its perturbation by temperature perturbation is unknown. As a result, the mean and perturbed dimensionless Henry's law constants are of 2 orders of magnitude difference, and this difference is overwhelmed by considerable large value of air diffusion coefficient. It is also worth noting that the revolatilization velocities in soil and water have been taken to be equal to the gas phase diffusive exchange velocities in the present study. Other expressions for the revolatilization velocities might be considered in the future (e.g., ref *28*). Because these velocities and partitioning coefficients are determined largely by chemical/physical properties of chemicals that exhibit considerable uncertainties, the model would inevitably result in errors in the predicted concentration perturbations.

Perturbation analysis provides a simple approach to examine anomalies of POPs as a departure from their mean, forced by climate change/variation (e.g., temperature). It cannot capture the complex coupling between meteorological variables involved in climate change nor handle spatial resolved variance of POPs while comparing with those box model and geographically resolved model scenarios (*9, 12*). In studying the relationship between climate change and POPs environmental fate, the current multimedia box models approximated numerically a sequence of time-invariant systems. The perturbation model predicts the variation of POPs and exchange in a two compartment system, and chemical/physical properties. It is therefore particularly useful for investigating the future trend of POPs perturbation in an ecosystem or in a region of interest under a specified or predicted climate change scenario (e.g., from the IPCC report, ref *1*).

The model developed in this study can be widely used in predicting the response of POPs to any climate change scenario in any region if mean concentrations in air and surface media can be provided. Projected climate scenarios can be obtained from gridded future air temperature and precipitation anomalies predicted by a General Circulation Model (GCM, ref *1*). The perturbation of chemical/physical properties and environmental parameters, such as the Henry's law constant, logK_{OA}, logK_{OW}, and degradation rate constants in multicompartments presented in SI can be employed in numerical assessment of long-range transport potentials of POPs (*24–26*) and contamination potentials (*29, 30*). The perturbation model is a useful tool to diagnose and screen the sensitivity of POPs environmental fate and long-range transport potential to air temperature and precipitation induced by climate change and variability on seasonal, inter-annual, and decadal time scales, and to the perturbations of their chemical/physical properties. It is expected that the perturbation analysis can be also applied in a multimedia box model (e.g., *9, 12*) by implementing perturbed physical/

chemical properties of POPs to examine the response of POPs to changes in air temperature and precipitation.

To demonstrate the capability of the perturbation model in predicting the response of a persistent chemical to interannual climate variability, Figure S7 of SI presents the simulated air concentration perturbations of HCB in the air−soil system and detrended (or residual) time series of measured HCB at Eagle Harbor on the shore of Lake Superior (47° 27′ 47″ N, 88° 08′ 59″ W) in springs of 1992−2007. The mean spring air temperature (277.9 K) and spring temperature anomalies (departure from the mean), denoting climate induced temperature perturbations, over the Great Lakes were obtained from the National Centers for Environmental Prediction (NCEP) reanalysis (27). In the calculation, the mean concentration of HCB in air and soil was taken as 70 pg m^{-3} and 0.2 μg kg^{-1} (6, 7), respectively. A recent study has demonstrated that stronger climate signals might exist in the residual time series of air concentrations of some legacy OCPs (11). The simulated perturbation of HCB in air associates very well with the residual time series of measured spring HCB ($r = 0.71$, $p = 0.003$ using data from 1993 to 2007), as shown in Figure S7 of SI. This suggests that revolatilization/deposition between air and soils associated with changes in air temperature contributed strongly to the change in HCB in the Great Lakes environment and demonstrates that the simulated concentration perturbations induced by temperature anomalies captures well interannual climate signals in the measured time series of HCB. Application of the POPs perturbation model derived in the present study under climate warming conditions in the Arctic and the Great Lakes ecosystems is currently underway to evaluate the effect of warming trend on the environmental fate of POPs in a realistic environment.

Supporting Information Available

Expression of mean and perturbed chemical/physical properties and environmental parameters of the selected chemicals, analytic solution of eq 8 using initial conditions, effect of perturbed precipitation and primary emission, Figures and Tables labeled as SI. This material is available free of charge via the Internet at http://pubs.acs.org.

Literature Cited

(1) Intergovernmental Panel on Climate Change. Fourth Assessment Report: Climate Change 2007. Available at http://www.ipcc.ch/.

(2) McKone, T. E.; Daniels, J. I.; Goldman, M. Uncertainties in the link between global climate change and predicted health risks from pollution: Hexachlorobenzene (HCB) case study using a fugacity model. *Risk Anal.* **1996**, *16* (3), 377–393.

(3) Macdonald, R. W.; Mackay, D.; Li, Y. F.; Hickie, B. How will global climate change affect risks from long-range transport of persistent organic pollutants? *Human Ecol. Risk Assess.* **2003**, *9* (3), 643–60.

(4) Macdonald, R. W.; Harner, T.; Fyfe, J. Recent climate change in the Arctic and its impact on contaminant pathways and interpretation of temporal trend data. *Sci. Total Environ.* **2005**, *342*, 5–86.

(5) Noyes, P. D.; McElwee, M. K.; Miller, H. D.; Clark, B. W.; van Tiem, L. A.; Walcott, K. C.; Erwin, K. N.; Levin, E. D. The toxicology of climate change: Environmental contaminants in a warming world. *Environ. Int.* **2009**, *35*, 971–986.

(6) Ma, J.; Venkatesh, S.; Jantunen, L. Evidence of the impact of ENSO events on temporal trends of hexachlorobenzene air concentrations over the Great Lakes. *Sci. Total Environ.* **2003**, *313*, 177–184.

(7) Ma, J.; Hung, H.; Blanchard, P. B. How do climate fluctuations affect persistent organic pollutant distribution in North America? Evidence from a decade of air monitoring. *Environ. Sci. Technol.* **2004**, *38*, 2538–2543.

(8) Ma, J.; Li, Y. Interannual variation of persistent organic pollutants over the Great Lakes induced by tropical Pacific sea surface temperature anomalies. *J. Geophys Res.* **2006**, *111*, D04302,; 10.1029/2005JD006014.

(9) MacLeod, M.; Riley, W. J.; Mckone, T. E. Assessing the influence of climate variability on atmospheric concentrations of polychlorinated biphenyls using a Global-Scale Mass Balance Model (BETR-Global). *Environ. Sci. Technol.* **2005**, *39*, 6749–6756.

(10) Becker, S.; Hallsell, C. J.; Tych, W.; Kallenborn, R.; Su, Y.; Hung, H. Long-term trends in atmospheric concentrations of α- and γ-HCH in the Arctic provide insight into the effects of legislation and climatic fluctuations on contaminant levels. *Atmos. Environ.* **2008**, *42*, 8225–8233.

(11) Gao, H.; Ma, J.; Cao, Z.; Dove, A.; Zhang, L. Trend and climate signals in seasonal air concentration of organochlorine pesticides over the Great Lakes. *J. Geophys. Res.* **2010**; 10.1029/2009JD013627.

(12) Lamon, L.; von Waldow, H.; MacLeod, M.; Scheringer, M.; Marcomini, A.; Hungerbühler, K. Modeling the global levels and distribution of polychlorinated biphenyls in air under a climate change scenario. *Environ. Sci. Technol.* **2009**, *43*, 5818–5824.

(13) Dalla Valle, M.; Codato, E.; Marcomini, A. Climate change influence on POPs distribution and fate: A case study. *Chemosphere* **2007**, *67* (7), 1287–1295.

(14) Li, Y. F.; MacDonald, R. Sources and pathways of selected organochlorine pesticides to the Arctic and the effect of pathway divergence on HCH trends in biota: A review. *Sci. Total Environ.* **2005**, *342*, 87–106.

(15) Jacob, D. J.; Winner, D. A. Effect of climate change on air quality. *Atmos. Environ.* **2009**, *43*, 51–63.

(16) Bennett, D.; Kastenberg, W.; McKone, T. General formulation of characteristic time for persistent chemicals in a multimedia environment. *Environ. Sci. Technol.* **1999**, *33*, 503–509.

(17) Mackay, M. *Multimedia Environmental Models: The Fugacity Approach*; CRC Press: Boca Raton, FL, 2001.

(18) Bidleman, T. F.; McConnell, L. L. A review of field experiments to determine air-water gas exchange of persistent organic pollutants. *Sci. Total Environ.* **1995**, *159*, 101–117.

(19) Pankow, J. F.; Isabelle, L. M.; Asher, W. E. Trace organic compounds in rain. 1. Sampler design and analysis by adsorption thermal desorption (ATD). *Environ. Sci. Technol.* **1984**, *18*, 310–318.

(20) Lei, Y. D.; Wania, F. Is rain or snow a more efficient scavenger of organic chemicals? *Atmos. Environ.* **2004**, *38*, 3557–3571.

(21) McPhaden, M. J.; Zhang, D. Slowdown of the meridional overturning circulation in the upper Pacific Ocean. *Nature* **2002**, *415*, 603–608.

(22) Gu, D.; Philander, S. G. H. Interdecadal climate fluctuations that depend on exchanges between the tropics and extratropics. *Science* **1997**, *275*, 805–807.

(23) Holton, J. R. *An Introduction to Dynamic Meteorology*; Elsevier Academic Press: Boston, MA, 2004.

(24) Scheringer, M.; Jones, K. C.; Matthies, M.; Simonich, S.; van de Meent, D. Multimedia partitioning, overall persistence, and long-range transport potential in the context of POPs and PBT chemical assessments. *Integr. Environ. Assess. Manage.* **2009**, *5*, 557–576.

(25) Strobes, M.; Scheringer, M.; Hungerbuhler, K. Measures of overall persistence and the temporal remote state. *Environ. Sci. Technol.* **2004**, *38*, 5665–5673.

(26) Beyer, A.; Mackay, D.; Matthies, M.; Wania, F.; Webster, E. Assessing long-range transport potential of persistent organic pollutants. *Environ. Sci. Technol.* **2000**, *34*, 699–703.

(27) Kalney, E.; Kanamitsu, M.; Kistler, R.; Collins, W.; Deaven, D.; Gandin, L.; Iredell, L.; Saha, S.; White, G.; Woollen, J.; et al. The NCEP/NCAR reanalysis project. *Bull. Am. Meteorol. Soc.* **1996**, *77*, 437–471.

(28) Stocker, J.; Scheringer, M.; Wegmann, F.; Hungerbuhler, K. Modeling the effect of snow and ice on the global environmental fate and long-range transport potential of semivolatile organic compounds. *Environ. Sci. Technol.* **2007**, *41*, 6192–6198.

(29) Wania, F. Potential of degradable organic chemicals for absolute and relative enrichment in the Arctic. *Environ. Sci. Technol.* **2006**, *40*, 569–77.

(30) Meyer, T.; Wania, F. What environmental fate processes have the strongest influence on a completely persistent organic chemical's accumulation in the Arctic? *Atmos. Environ.* **2007**, *41*, 2757–2767.